JOURNAL OF GEOPHYSICAL RESEARCH, VOL. 112, D24S18, doi:10.1029/2007JD008728, 2007

Role of atmospheric aerosol concentration on deep convective precipitation: Cloud-resolving model simulations

Wei-Kuo Tao,[1] Xiaowen Li,[1,2] Alexander Khain,[3] Toshihisa Matsui,[1,2] Stephen Lang,[4] and Joanne Simpson[1]

Received 30 March 2007; revised 28 September 2007; accepted 22 October 2007; published 22 December 2007.

[1] A two-dimensional cloud-resolving model with detailed spectral bin microphysics is used to examine the effect of aerosols on three different deep convective cloud systems that developed in different geographic locations: south Florida, Oklahoma, and the central Pacific. A pair of model simulations, one with an idealized low cloud condensation nuclei (CCN) (clean) and one with an idealized high CCN (dirty environment), is conducted for each case. In all three cases, rain reaches the ground earlier for the low-CCN case. Rain suppression is also evident in all three cases with high CCN. However, this suppression only occurs during the early stages of the simulations. During the mature stages of the simulations the effects of increasing aerosol concentration range from rain suppression in the Oklahoma case to almost no effect in the Florida case to rain enhancement in the Pacific case. The model results suggest that evaporative cooling in the lower troposphere is a key process in determining whether high CCN reduces or enhances precipitation. Stronger evaporative cooling can produce a stronger cold pool and thus stronger low-level convergence through interactions with the low-level wind shear. Consequently, precipitation processes can be more vigorous. For example, the evaporative cooling is more than two times stronger in the lower troposphere with high CCN for the Pacific case. Sensitivity tests also suggest that ice processes are crucial for suppressing precipitation in the Oklahoma case with high CCN. A comparison and review of other modeling studies are also presented.

Citation: Tao, W.-K., X. Li, A. Khain, T. Matsui, S. Lang, and J. Simpson (2007), Role of atmospheric aerosol concentration on deep convective precipitation: Cloud-resolving model simulations, *J. Geophys. Res.*, *112*, D24S18, doi:10.1029/2007JD008728.

1. Introduction

[2] Aerosols and especially their effect on clouds are one of the key components of the climate system and the hydrological cycle [*Ramanathan et al.*, 2001]. Yet, the aerosol effect on clouds remains largely unknown and the processes involved not well understood. A recent report published by the National Academy of Science states "The greatest uncertainty about the aerosol climate forcing—indeed, the largest of all the uncertainties about global climate forcing—is probably the indirect effect of aerosols on clouds" [*National Research Council*, 2005, p. 29]. The aerosol effect on clouds is often categorized into the traditional "first indirect (i.e., Twomey)" effect on the cloud droplet sizes for a constant liquid water path [*Twomey*, 1977] and the "semidirect" effect on cloud coverage [e.g., *Ackerman et al.*, 2000]. Enhanced aerosol concentrations can also suppress warm rain processes by producing a narrow droplet spectrum that inhibits collision and coalescence processes [e.g., *Squires and Twomey*, 1960; *Warner and Twomey*, 1967; *Warner*, 1968; *Rosenfeld*, 1999].

[3] The aerosol effect on precipitation processes, also known as the second type of aerosol indirect effect [*Albrecht*, 1989], is even more complex, especially for mixed-phase convective clouds. A combination of cloud top temperature and effective droplet sizes, estimated from the Advanced Very High Resolution Radiometer (AVHRR), has been used to infer the suppression of coalescence and precipitation processes for smoke [*Rosenfeld and Lensky*, 1998] and desert dust [*Rosenfeld et al.*, 2001]. Multisensor (passive/active microwave and visible and infrared sensors) satellite observations from the Tropical Rainfall Measuring Mission (TRMM) have been used to infer the presence of nonprecipitating supercooled liquid water near the cloud top due to overseeding from both smoke over Indonesia [*Rosenfeld*, 1999] and urban pollution over Australia [*Rosenfeld*, 2000]. In addition, aircraft measurements have provided evidence of sustained supercooled liquid

[1]Laboratory for Atmospheres, NASA Goddard Space Flight Center, Greenbelt, Maryland, USA.
[2]Goddard Earth Sciences and Technology Center, University of Maryland, Baltimore County, Baltimore, Maryland, USA.
[3]Department of Atmospheric Science, Hebrew University of Jerusalem, Jerusalem, Israel.
[4]Science Systems and Applications, Inc., Lanham, Maryland, USA.

0148-0227/07/2007JD008728$09.00

Table 1. Key Observational Studies Identifying the Differences in the Microphysical Properties, Cloud Characteristics, Thermodynamics, and Dynamics Associated With Clouds and Cloud Systems Developed in Dirty and Clean Environments

Properties	High CCN (Dirty)	Low CCN (Clean)	References (Observations)
Cloud droplet size distribution	narrower	broader	*Rosenfeld and Lensky* [1998], *Rosenfeld* [1999, 2000], *Rosenfeld et al.* [2001], *Rosenfeld and Woodley* [2000], *Andreae et al.* [2004], *Koren et al.* [2005],
Warm-rain process	suppressed	enhanced	*Rosenfeld* [1999, 2000], *Rosenfeld and Woodley* [2000], *Rosenfeld and Ulbrich* [2003], *Andreae et al.* [2004], *Lin et al.* [2006]
Cold-rain process	enhanced	suppressed	*Rosenfeld and Woodley* [2000], *Orville et al.* [2001], *Williams et al.* [2002], *Andreae et al.* [2004], *Lin et al.* [2006], *Bell et al.* [2007]
Mixed phase region	deeper	shallower	*Rosenfeld and Lensky* [1998], *Williams et al.* [2002], *Lin et al.* [2006]
Cloud top height	higher	lower	*Andreae et al.* [2004], *Koren et al.* [2006], *Lin et al.* [2006]
Lightning	enhanced (downwind side)/higher max flash	less and lower max flash	*Williams et al.* [2002], *Orville et al.* [2001]

water down to −37.5°C in continental mixed-phase convective clouds [*Rosenfeld and Woodley*, 2000]. These findings further suggest that continental aerosols reduce the mean size of cloud droplets, suppressing coalescence and warm rain processes, permitting more freezing of cloud droplets and associated latent heat release above the 0°C isotherm, and enhancing the growth of large hail and cold rain processes [*Rosenfeld and Woodley*, 2000]. *Andreae et al.* [2004] analyzed in situ observation during LBA-SMOCC (the Large-Scale Biosphere-Atmosphere Experiment in Amazonia-Smoke, Aerosols, Clouds, Rainfall, and Climate) campaign and found that increases in smoke and surface heat due to biomass burning tend to lead to higher cloud top heights and the enhancement of cold rain processes over the Amazon basin. *Lin et al.* [2006] examined multiplatform satellite data over the Amazon basin and found that high biomass burning-derived aerosols are correlated with the high cloud top heights, large anvils, and more rainfall. *Koren et al.* [2005] examined cloud properties derived from the Moderate Resolution Imaging Spectroradiometer (MODIS) and found strong evidence that aerosols from pollution, desert dust and biomass burning systematically invigorate convective clouds over the Atlantic Ocean. Using long-term integrated TRMM-derived precipitation data, *Bell et al.* [2007] found a significant midweek increase in summertime afternoon thunderstorms over the southeast U.S., which coincides with a midweek increase in ground-measured aerosol concentration. These findings are consistent with the notion that aerosols have a major impact on the dynamics, microphysics, and electrification properties of continental mixed-phase convective clouds [*Rosenfeld and Woodley*, 2000; *Orville et al.*, 2001; *Williams et al.*, 2002]. In addition, high aerosol concentrations in urban environments could affect precipitation variability by providing an enhanced source of cloud condensation nuclei (CCN). Hypotheses have been developed to explain the effect of urban regions on convection and precipitation [*van den Heever and Cotton*, 2007; *Shepherd*, 2005].

[4] Table 1 summarizes the key observational studies identifying the microphysical properties, cloud characteristics, thermodynamics and dynamics associated with cloud systems from high-aerosol continental environments. For example, atmospheric aerosol concentrations can influence cloud droplet size distributions, warm rain process, cold rain process, cloud top height, the depth of the mixed phase region, and occurrence of lightning. These observational studies are useful for validating modeling studies.

[5] Recently, cloud-resolving models (CRMs) have been used to examine the role of aerosols on mixed-phase convective clouds (see Table 2). These modeling studies had many differences in terms of model configuration (two-dimensional (2-D) or 3-D), domain size, grid spacing (150–3000 m), microphysics (i.e., two-moment bulk, simple or sophisticated spectral bin), turbulence (first- or 1.5-order TKE), radiation, lateral boundary conditions (i.e., closed, radiative open and cyclic), cases (isolated convection, tropical/midlatitude squall lines) and model integration time (e.g., 2.5 to 48 h). Almost all of the model results indicated that aerosol concentration had a significant impact on precipitation processes. For example, *Khain and Pokrovsky* [2004] and *Khain et al.* [2004, 2005] found that an increase in aerosol concentration (or CCN) reduced precipitation processes (and rainfall) for both an East Atlantic squall line and a Texas convective cloud. They also found that an increase in CCN enhanced precipitation for an Oklahoma squall line. *Khain et al.* [2004, 2005] found that aerosol effects on precipitation for deep convective clouds strongly depend on relative humidity and the environmental conditions, so that an increase in aerosol concentration for maritime tropical convection can lead to an increase in precipitation amount. In addition, they reported that aerosols could affect the dynamics of convection via the strength of convective updrafts and downdrafts [*Khain et al.*, 2004], fostering the formation of secondary clouds in squall lines and thus increasing precipitation. On the other hand, *Wang* [2005] found that precipitation could either be enhanced or reduced by increasing the CCN for a squall line that developed in the ITCZ (Intertropical Convergence Zone). *Fan et al.* [2007] found that ice microphysics, clouds and precipitation changed considerably with aerosol chemical properties for a convective event in Houston, Texas. *Fridlind et al.* [2004] found midtropospheric aerosols were important as subtropical anvil nuclei for an isolated cloud, but *Khain and Pokrovsky* [2004] and *van den Heever and Cotton* [2007] indicated that lower tropospheric aerosols (penetrating cloud base and below 4 km) dominated for deep convective clouds. These differences could be due to model physics, cases and/or setups (e.g., domain size, lateral boundary conditions). *Teller and Levin* [2006] showed that high CCN concentrations reduced precipitation in mixed-phase convective clouds during the first hour of model integration.

Table 2. Key Papers Using CRMs to Study the Impact of Aerosols on Precipitation[a]

	Dimensions	Microphysics	Turbulence	Radiation	Domain	Grid Size and Time Step	Lateral Boundary Conditions	Cases	Integration
Khain et al. [2004]	2-D	spectral bin (33 bin); 6 types of ice	first order	no	64 × 16 km	dx = 250 m, dz = 125 m, dt = 5 s	closed	squall lines (E. Atlantic) and a convective cloud (Texas)	~2 h
Khain and Pokrovsky [2004]	2-D	spectral bin (33 bin); 6 types of ice	first order	no	64 × 16 km	dx = 250 m, dz = 125 m, dt = 5 s	closed	a convective cloud (Texas)	2.5 h
Khain et al. [2005]	2-D	spectral bin (33 bin); 6 types of ice	first order	no	128 × 16 km	dx = 250 m, dz = 125 m, dt = 5 s	closed	two squall lines (E. Atlantic and Oklahoma) and a convective cloud (Texas)	2 and 4 h
Fridlind et al. [2004]	3-D	spectral bin (16 bins); 1 type of ice	first order	no	48 × 48 × 24 km	dx = dy = 500 m, dz = 375 m, dt = 5 s	closed	a convective cloud (Florida)	3 h
Wang [2005]	3-D	two-moment bulk scheme	first order	6 broadbands for solar and 12 for IR; four-stream discrete-ordinate scattering, k-distribution	400 × 200 × 25 km	dx = dy = 2000 m, dz = 500 m, dt = 5 s	cyclic	a squall line (ITCZ)	4 h
van den Heever et al. [2006]	3-D	two-moment bulk scheme	first order	a broadband two-stream for solar and an emissivity for IR	145 × 145 × 20 km	dx = dy = 500 m, dz = stretched, dt = 1 s	radiative open	thunderstorm (CRYSTAL-FACE)	1 2 h
Cheng et al. [2007]	3-D	two-moment bulk scheme (warm rain only)	first order	a simple broadband solar and emissivity (IR)	810 × 810 km × 100 Pa	dx = dy = 3000 m, dz = stretched, dt = 5 s	radiative open	a shallow Stratus (ARM-SGP)	72 h
Lynn et al. [2005a, 2005b]	3-D	spectral bin (33 bin); 3 types of ice and bulk scheme	TKE	A broadband two-stream for solar and an emissivity for IR	400 × 199 × 25 km	dx = dy = 1000 m, dz = stretched, dt = 9 s	radiative open	a squall line (Florida)	13 h
Fan et al. [2007]	2-D	spectral bin (33 bin); 6 types of ice	TKE	no	512 × 22 km	dx = 500 m, dz = stretched (250–1260 m), dt = 6 s	radiative open	a sea breeze–induced convective event (Houston, Tx)	3 h
Teller and Levin [2006]	2-D	spectral bin (33 bin); 3 types of ice	first order	no	30 × 8 km	dx = 300 m, dz = 300 m, dt = 2 s	closed	winter convective cloud eastern Mediterranean	80 min
van den Heever and Cotton [2007]	3-D	two-moment bulk scheme	first order	a broadband two-stream for solar and an emissivity for IR	228 × 228 × 22 km	dx = dy = 1500 m, dz = stretched, dt = 2 s	radiative open	thunderstorm (St. Louis)	26 h

[a]Model dimensionality (2-D or 3-D), microphysical schemes (spectral bin or two-moment bulk), turbulence parameterization (first- or 1.5-order TKE), radiation (with or without), domain size (km), resolution (m), time step (s), lateral boundary condition (closed, cyclic, or radiative open), and case and integration time (h) are all listed.

[6] Regional-scale models with fine resolution have also been used to study the impact of aerosols on precipitation [i.e., *van den Heever et al.* 2006; *van den Heever and Cotton*, 2007; *Lynn et al.*, 2005a, 2005b; *Cheng et al.*, 2007]. For example, *Lynn et al.* [2005b] found a "continental" aerosol concentration produces a larger earlier maximum rainfall rate and more accumulated rainfall than does a "maritime" aerosol concentration for a squall line; however, time accumulated rain is slightly larger with a maritime aerosol concentration over the whole model domain. *Cheng et al.* [2007] found that increasing aerosols inhibited precipitation for an Oklahoma warm cloud system. *van den Heever et al.* [2006] found that high-GCCN (giant CCN) and −IN (ice nuclei) cases initially enhance the surface precipitation during the first 6 h of integration because of initial broadening of the cloud droplet spectra, whereas high CCN reduce total accumulated precipitation. *van den Heever and Cotton* [2007] found that the response of convective rainfall to urban-enhanced aerosols becomes stronger when the background aerosol concentrations are low.

[7] In almost all cases, idealized aerosol concentrations were used in the model simulations. Aerosol concentrations observed/measured from a previous day were used by *Fridlind et al.* [2004]. Vertical profiles of CCN, GCCN, and ice forming nuclei (IFN) obtained on "dirty" and "clean" days during the CRYSTAL-FACE (Cirrus Regional Study of Tropical Anvils and Cirrus Layers−Florida Area Cumulus Experiment) were used by *van den Heever et al.* [2006] and *van den Heever and Cotton* [2007] as benchmarks for their model sensitivity tests. Furthermore, almost none of these CRM studies compared the model results with observed cloud structures, organization, radar reflectivity and rainfall. Some of the CRM domains were too small to resolve the observed clouds or precipitation systems (the domain size has to be at least twice as large as the simulated features).

[8] This paper will investigate the effect of atmospheric aerosols on precipitation processes using a 2-D CRM with detailed spectral bin microphysics. Three different cloud systems with very different environmental conditions will be simulated. Sensitivity tests will be conducted to examine the precipitation processes associated with dirty and clean environments. The model and three cases will be described in section 2. The results and comparison with previous modeling studies will be discussed in sections 3 and 4, respectively. In section 5, the summary and future work will be presented.

2. Model and Cases

2.1. Model Description

[9] The model used in this study is the 2-D version of the Goddard Cumulus Ensemble (GCE) model. The GCE model was originally developed by *Soong and Ogura* [1980] and *Soong and Tao* [1980]. The equations that govern the cloud-scale motion are anelastic by filtering out sound waves. The subgrid-scale turbulence used in the model is based on work by *Klemp and Wilhelmson* [1978]. In their approach, one prognostic equation is solved for subgrid kinetic energy, which is then used to specify the eddy coefficients. The effect of condensation on the generation of subgrid-scale kinetic energy is also incorporated to the model [*Soong and Ogura*, 1980]. The model includes interactive solar [*Chou et al.*, 1998] and thermal infrared [*Chou and Suarez*, 1994] radiation parameterization schemes. All scalar variables (potential temperature, mixing ratio of water vapor, turbulence coefficients, and all hydrometeor classes) use forward time differencing and a positive definite advection scheme with a nonoscillatory option [*Smolarkiewicz and Grabowski*, 1990]. The dynamic variables, u and w, use a fourth-order accurate advection scheme and leapfrog time integration. Details of the GCE model description and improvements can be found in work by *Tao and Simpson* [1993] and *Tao et al.* [2003a].

[10] The spectral bin microphysics used in the GCE model were developed by *Khain et al.* [2000], *Khain et al.* [2004], and *Khain et al.* [2005]. The formulation is based on solving stochastic kinetic equations for the size distribution functions of water droplets (cloud droplets and raindrops), and six types of ice particles: pristine ice crystals (columnar and plate-like), snow (dendrites and aggregates), graupel, and frozen drops/hail. Each type is described by a size distribution using 33 categories (mass bins). Size spectra of atmospheric aerosols are also described using 33 bins.

[11] The spectral bin microphysics includes the following processes: (1) nucleation of droplets and ice particles [*Pruppacher and Klett*, 1997; *Meyers et al.*, 1992], (2) immersion freezing [*Vali*, 1994], (3) ice multiplication [*Hallett and Mossop*, 1974; *Mossop and Hallett*, 1974], (4) detailed melting [*Khain et al.*, 2004], (5) condensation/evaporation of liquid drops [*Pruppacher and Klett*, 1997; *Khain et al.*, 2000], (6) deposition/sublimation of ice particles [*Pruppacher and Klett*, 1997; *Khain et al.*, 2000], (7) drop/drop, drop/ice, and ice/ice collision/coalescence [*Pruppacher and Klett*, 1997; *Pinsky et al.*, 2001], (8) turbulence effects on liquid drop collisions [*Pinsky et al.*, 2000], and (9) collisional breakup [*Seifert et al.*, 2005]. In the first process, both condensation-freezing and homogeneous nucleation are considered. The Meyers' formula is applied in a semi-Lagranigan approach [see *Khain et al.*, 2000]. The concentration of newly nucleated ice crystals at each time step is calculated by the increase in the value of supersaturation. Sedimentation of liquid and ice particles is also considered. This model is specially designed to take into account the effect of atmospheric aerosols on cloud development and precipitation formation. The activation of aerosols in each size bin are explicitly calculated in this scheme [*Khain et al.*, 2000].

[12] The initial aerosol size distribution is calculated with an empirical formula: $N = N_0 S_w^k$ [*Pruppacher and Klett*, 1997], where S_w is the supersaturation with respect to water and N_0 and k are constants. The formula gives the size distribution of the initial CCN spectrum. In this study, the baseline simulations (clean scenarios) use $N_0 = 100\ cm^{-3}$ and k = 0.42 for the clean maritime (TOGA COARE) case, and $N_0 = 600\ cm^{-3}$ and k = 0.3 for the clean continental (PRESTORM and CRYSTAL) cases [*Twomey and Wojciechowski*, 1969]. The dirty scenarios for all three cases assume $N_0 = 2500\ cm^{-3}$ and k = 0.3. In continental cases, aerosols with diameters larger than 0.8 μm are removed [*Cooper et al.*, 1997]. The oceanic aerosols have plenty of large size aerosols generated from sea spray, but they do not have very fine particles [*Hudson*, 1984, 1993].

Table 3. Initial Environmental Conditions Expressed in Terms of Convective Available Potential Energy and Precipitable Water for the TOGA COARE, PRESTORM and CRYSTAL-FACE Cases[a]

	Location	System Type	CAPE, $m^2\ s^{-2}$	Precipitable Water, $g\ cm^{-2}$	References
TOGA COARE (22 Feb 1993)	Tropical Pacific	MCS	1776	6.334	*Wang et al.* [1996, 2003], *Tao et al.* [2003a], *Lang et al.* [2003]
PRESTORM (10–11 Jun 1985)	Oklahoma	MCS	2300	4.282	*Tao et al.* [1995, 1996], *Lang et al.* [2003]
CRYSTAL-FACE (16 Jul 2002)	Florida	sea breeze convection	2027	4.753	this paper

[a]The geographic locations, storm type, and previous modeling papers are also shown. CAPE is convective available potential energy.

Therefore small CCN, which can only be activated when the ambient super saturation exceeds 1.1%, are eliminated from the maritime aerosol spectra.

[13] Radiative open lateral boundary conditions are used [*Klemp and Wilhelmson*, 1978]. A large horizontal domain is used in this study to simulate the large convective system and minimize the reflection of convectively generated gravity waves at the lateral boundaries [see *Fovell and Ogura*, 1988]. At the top of the model, a free-slip condition is used for horizontal wind, temperature, and specific humidity, and zero vertical velocity is applied. There are 1024 horizontal grid points with a resolution of 1 km in the center 720 points and stretched grids on either side. Use of the stretched horizontal grid makes the model less sensitive to the choice of gravity wave speed associated with the open lateral boundary conditions [*Fovell and Ogura*, 1988]. For the present study, a stretched vertical coordinate with 33 levels is used. The model has finer resolution (about 80 m) in the boundary layer and coarser resolution (about 1000 m) in the upper levels. The model time step is 5 s.

2.2. Cases

[14] Three cases, a tropical oceanic squall system observed during TOGA COARE (Tropical Ocean and Global Atmosphere Coupled Ocean-Atmosphere Response Experiment, which occurred over the Pacific Ocean warm pool from November 1992 to February 1993), a midlatitude continental squall system observed during PRESTORM (Preliminary Regional Experiment for STORM-Central, which occurred in Kansas and Oklahoma during May–June 1985), and a midafternoon convection observed during CRYSTAL-FACE (Cirrus Regional Study of Tropical Anvils and Cirrus Layers–Florida Area Cumulus Experiment, which occurred in Florida during July 2002), will be used to examine the impact of aerosols on deep, precipitating systems. The 10–11 June 1985 PRESTORM case has been well studied [e.g., *Johnson and Hamilton*, 1988; *Rutledge et al.*, 1988; *Tao et al.*, 1995, 1996; *Yang and Houze*, 1995; *Lang et al.*, 2003]. The PRESTORM environment is fairly unstable and relatively dry. The model is initialized with a single sounding taken at 2330 UTC from Pratt, KS, which is ahead of the squall line. The sounding has a lifted index of −5.37 and a convective available potential energy (CAPE) of 2300 J/kg. Radiation is included but not surface fluxes. The convective system is initiated using a low-level cold pool.

[15] The 22 February 1993 TOGA COARE squall line has also been well studied [*Jorgensen et al.*, 1997; *Redelsperger et al.*, 2000; *Trier et al.*, 1996, 1997; *Wang et al.*, 1996, 2003]. The sounding used to initialize the model is from *LeMone et al.* [1994]. It is a composite of aircraft data below 6 km and an average of the 1800 and 2400 UTC Honiara soundings above 6 km. The CAPE and lifted index are moderately unstable, 1776 J/kg and −3.2, respectively. Surface fluxes are included in the model for this case using the TOGA COARE flux algorithm [*Fairall et al.*, 1996; *Wang et al.*, 1996]. The vertical grids are similar to the PRESTORM setup, but with the first grid of 40 m to accommodate the TOGA COARE flux algorithm. The horizontal grids follow that of PRESTORM, but with an inner resolution of 750 m. Radiation is included, and a low-level cold pool is used to start the system. Low-level mesoscale lifting is also applied. It has a peak value of 3.4 cm/s near 1 km and is applied over the first 2 h. Note that the mesoscale model simulations [*van den Heever et al.*, 2006; *van den Heever and Cotton*, 2007; *Lynn et al.*, 2005a, 2005b] can explicitly represent mesoscale forcing/lifting (e.g., sea breeze convergence and urban heat island convergence).

[16] Both the TOGA COARE and PRESTORM cases are well-organized and long-lived mesoscale convective systems. The CRYSTAL-FACE 16 July 2002 case is a sea breeze convection case that developed over south Florida [*Ridley et al.*, 2004; *Heymsfield et al.*, 2004]. It originated near the coast and propagated inland and dissipated within a couple of hours. This storm generated a large anvil and had good aircraft measurements in terms of cloud chemistry. The CAPE, total precipitable water, Lifted Index are 2027 J/kg, 4.753 g/cm^2 and −4.23, respectively, which are lower and more moist than the PRESTORM case but higher and drier than the TOGA COARE case. The local sounding and wind profile at the West Coast ground site (located at the Everglades National Park Gulf Coast Visitor Center) taken previous to the onset of convection at 1731 UTC is used in this simulation. The convection is initialized using three warm bubbles 40 km apart with a maximum temperature perturbation of 6 K and water vapor perturbation of 6 g/kg. The rest of the model setup and physics are the same as the PRESTORM case. Table 3 shows some characteristics of the environmental conditions associated with these three cases.

3. Results

[17] Figure 1 shows the observed and simulated radar reflectivity for the TOGA COARE, PRESTORM and

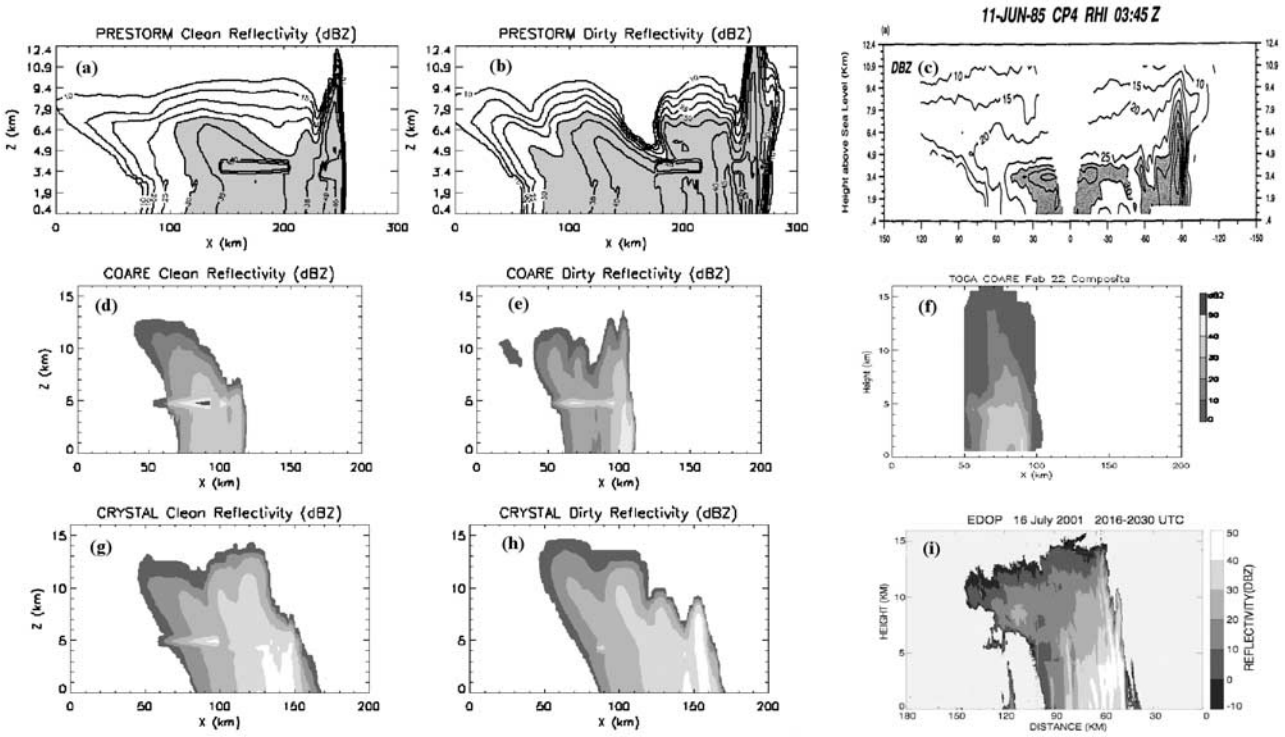

Figure 1. Observed and simulated radar reflectivity for the PRESTORM, TOGA COARE, and CRYSTAL-FACE cases under dirty and clean conditions: (a) PRESTORM clean, (b) PRESTORM dirty, (c) PRESTORM observed (adapted from *Rutledge et al.* [1988]), (d) TOGA COARE clean, (e) TOGA COARE dirty, (f) TOGA COARE observed (courtesy of D. Jorgensen from NOAA National Severe Storms Laboratory), (g) CRYSTAL clean, (h) CRYSTAL dirty, and (i) CRYSTAL observed (courtesy of J. Heymsfield from NASA Goddard Space Flight Center).

CRYSTAL-FACE cases with dirty and clean conditions. The model simulations capture the various storm sizes and structures in the different environmental conditions quite well. For example, the leading convection and the extensive trailing stratiform rain area compare well with the radar reflectivity observed during the mature stage of the continental PRESTORM case [*Rutledge et al.*, 1988]. Clean cases (i.e., the control experiments) generally agree better with the observations. In terms of radar reflectivity magnitudes, the agreement between the simulations and observations is better at lower levels where only liquid phase cloud/rainwater exists. The simulated radar reflectivity tends to be higher at upper levels and in the anvil area where ice phase particles dominate. This is partly due to the simplified assumption of uniform snow densities in this calculation. The melting band signal is also amplified by assuming that all of the melting particles are coated by a layer of water on their surfaces.

[18] Figure 2 shows time sequences of the GCE model-estimated domain mean surface rainfall rate for the PRESTORM, TOGA COARE and CRYSTAL cases. Rain suppression in the high CCN concentration (i.e., dirty environment) runs is evident in all three case studies but only during the first hour of the simulations. Rain reaches the ground early in all the clean cases. This is in good agreement with observations [e.g., *Rosenfeld*, 1999, 2000]. During the mature stage of the simulations, the effect of increasing the CCN concentration ranges from rain suppression in the PRESTORM case to little effect in the CRYSTAL-FACE case to rain enhancement in the TOGA COARE case. These results suggest that model simulations of the whole life cycle of convective system are needed in order to assess the impact of aerosols on precipitation processes associated with mesoscale convective systems and thunderstorms. These results also show the complexity of aerosol-cloud-precipitation interaction within deep convection.

[19] Table 4 shows the domain-averaged surface rainfall amounts, stratiform percentages, precipitation efficiencies, and ice water path ratios (ice water path divided by the sum of the liquid and ice water paths) for the TOGA COARE, PRESTORM and CRYSTAL-FACE cases under clean and dirty conditions. The precipitation is divided into convective and stratiform components [*Tao et al.*, 1993; *Lang et al.*, 2003]. The convective region includes areas with strong vertical velocities (over 3–5 m s^{-1}) and/or heavy surface rainfall. The stratiform region is simply nonconvective. For the PRESTORM case, the dirty scenario produces more stratiform (light) precipitation than does the clean case. It is expected that a high CCN concentration allows for more small cloud droplets and ice particles to form. The lower collection coefficient for smaller cloud and ice particles allows for a larger amount of ice phase particles to be transported into the trailing stratiform region, producing a

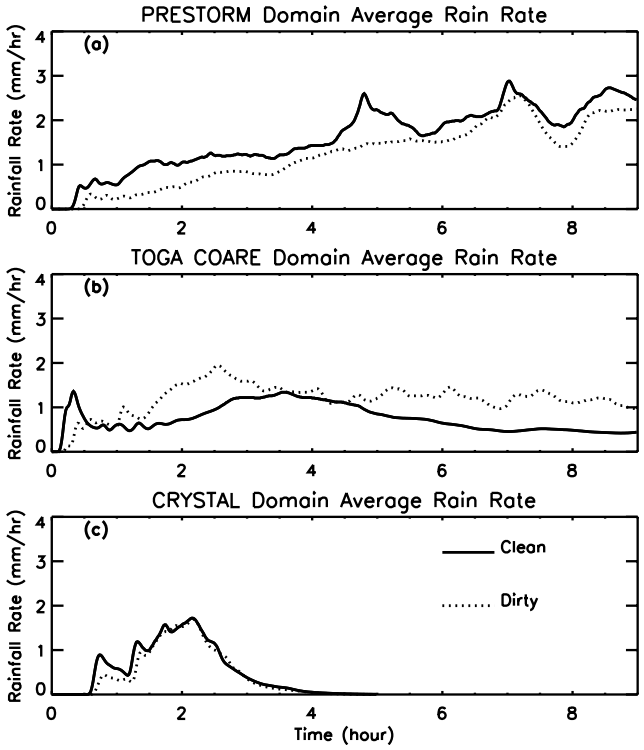

Figure 2. Time series of GCE model-estimated domain mean surface rainfall rate (mm h^{-1}) for the (a) PRESTORM, (b) TOGA COARE, and (c) CRYSTAL cases. The solid (dashed) line represents clean (dirty) conditions.

higher stratiform rain percentage in the dirty case. Aerosols do not have much impact on the stratiform percentage for the CRYSTAL-FACE case because of its short life span. The reduction in stratiform rain (or light rain) in the dirty environment for the TOGA COARE case is due to its enhanced convective activity (stronger updrafts).

[20] Precipitation efficiency (PE) is an important physical parameter for measuring the interaction between convection and its environment. Its definition varies [e.g., *Ferrier et al.*, 1996; *Sui et al.*, 2007]. In this study, the precipitation efficiency is defined as PE = (P − L)/P, where P is the total mass of condensates formed in clouds by diffusional growth, and L is the loss of condensate mass due to drop evaporation and ice sublimation. The same precipitation efficiency was used by *Khain et al.* [2005]. When total evaporation and sublimation are very small, PE will be close to 1. Smaller PE generally indicates more evaporation/sublimation (i.e., during the decaying or less active stage of clouds/cloud systems). The PEs of cloud systems in drier environments (e.g., PRESTORM and CRYSTAL-FACE) are generally smaller than those in moist environments (e.g., TOGA COARE). In addition, the simulations with a dirty environment have a smaller PE than their counterparts for all three cases. This is because the smaller cloud droplets/ice particles simulated in the dirty cases result in larger evaporation/sublimation. Even for the TOGA COARE case, where increasing the aerosols enhanced total surface rain, the relative increase of evaporation in the dirty scenario still outweighs the relative enhancement of diffusional growth, resulting in a decrease in precipitation efficiency. For example, in the definition $dPE \propto \frac{dP}{P} - \frac{dL}{L}$, domain average $\frac{dP}{P} = 0.45$ while $\frac{dL}{L} = 0.66$, indicating a higher sensitivity of evaporation to increasing aerosol concentrations compared with the total condensation in this rain enhanced case. Table 4 also shows higher ice water path ratios for the continental cloud systems (i.e., PRESTORM and CRYSTAL-FACE). The larger CAPE and stronger convective updrafts in the PRESTORM and CRYSTAL-FACE produce more ice particles than in the TOGA COARE case.

[21] For the PRESTORM and CRYSTAL-FACE cases, the PE in the dirty run is only 7% and 5% smaller, respectively, than in the clean run. The strengths of the convective updrafts vary little between the dirty and clean scenarios for both cases (Figure 3). This could be the reason for the small changes in PE between the dirty and clean runs and could also account for the similarity in their ice water paths. The PE is reduced by 13% in the dirty scenario for the TOGA COARE case. The much stronger convective activity simulated in the dirty case produces a wider and deeper anvil and more ice sublimation. This may be the cause of smaller PE in the dirty case. This also shows that the dirty environment leads to more ice formation for TOGA COARE.

[22] Figure 3 shows time sequences of GCE model-simulated maximum vertical velocity for PRESTORM, TOGA COARE and CRYSTAL-FACE. The maximum vertical velocity is stronger in PRESTORM than in both TOGA COARE and CRYSTAL because PRESTORM has the largest CAPE. *Williams et al.* [2002] suggested that updraft strength would be stronger in a dirty environment. For both PRESTORM and CRYSTAL, the maximum ver-

Table 4. Domain-Averaged Surface Rainfall Amount, Stratiform Percentage, Precipitation Efficiency, and Ice Water Path Ratio for the TOGA COARE, PRESTORM, and CRYSTAL-FACE Cases Under Dirty and Clean Conditions[a]

	TOGA COARE Clean (100)	TOGA COARE Dirty (2500)	PRESTORM Clean (600)	PRESTORM Dirty (2500)	CRYSTAL Clean (600)	CRYSTAL Dirty (2500)
Averaged rain (mm/d/grid), mm d^{-1}	18.0	28.4	38.3	29.1	12.6	11.0
Stratiform, %	50	17	43	70	43	40
Precipitation efficiency, %	65	52	33	26	33	28
Ice water path ratio[b]	.52	.65	.86	.88	.75	.79

[a]Note there are 9 h in the PRESTORM and TOGA COARE simulations and 5 h in the CRYSTAL-FACE simulation.
[b]Ice water path ratio is ice water path divided by the total liquid and ice water path.

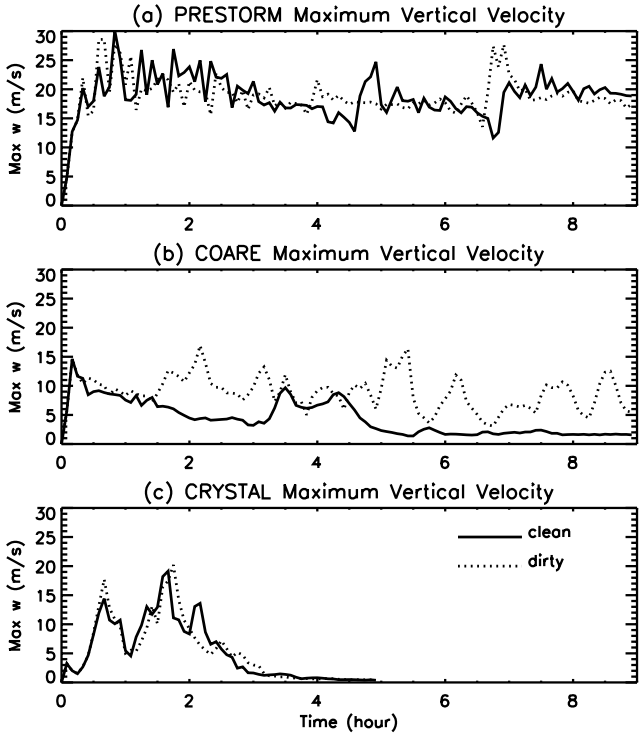

Figure 3. Time series of GCE model-simulated maximum vertical velocity (m s^{-1}) for the (a) PRESTORM, (b) TOGA COARE, and (c) CRYSTAL cases. The solid (dashed) line represents clean (dirty) conditions.

tical velocity for the dirty scenario is slightly stronger than the clean environment during the early stages of storm development. However, aerosols do not have a major influence on the maximum vertical velocities in these two continental cases. Note that the updrafts (both maximum and domain averaged) are slightly stronger as the aerosol concentrations are increased for the 28 July 2002 (CRYSTAL –FACE) case as simulated by *van den Heever et al.* [2006]. The differences in initialization between the present study and *van den Heever et al.* [2006] could be one of the major reasons for the difference in cloud updraft strength. Other reasons could be the dimensionalities (3-D versus 2-D) and environmental conditions. The TOGA COARE case, on the other hand, shows much stronger maximum vertical velocities with a high CCN concentration (dirty environment). This is consistent with the increase in simulated surface precipitation. The maximum vertical velocities do not vary between the dirty and clean runs in the early stages of the TOGA COARE case.

[23] Figure 4 shows probability distribution functions (PDFs) of rainfall intensity for the PRESTORM, TOGA COARE and CRYSTAL cases during the first hour of simulation. All three cases produce more light rain in the dirty environment. However, over the entire 9-h simulation, only the PRESTORM case maintains this characteristic. In TOGA COARE, more light precipitation was simulated in the clean case, contrary to the first hour results, because simulated vertical velocities are weaker with a low CCN (see Figure 3b). The cumulated surface rainfall PDFs for the clean and dirty scenarios do not differ significantly over the 5-h storm duration in CRYSTAL.

[24] *Rosenfeld and Lensky* [1998] suggested that a deeper mixed-phase layer may exist in dirty environments (high CCN). *Williams et al.* [2002] and *Andreae et al.* [2004] also suggested that higher maximum lightning flash rates associated with more mixed phase processes would occur for dirty environments. In this study, additional model sensitivity experiments were performed by turning off the ice processes to examine the impact of ice microphysics on the aerosol-precipitation interactions. In these sensitivity

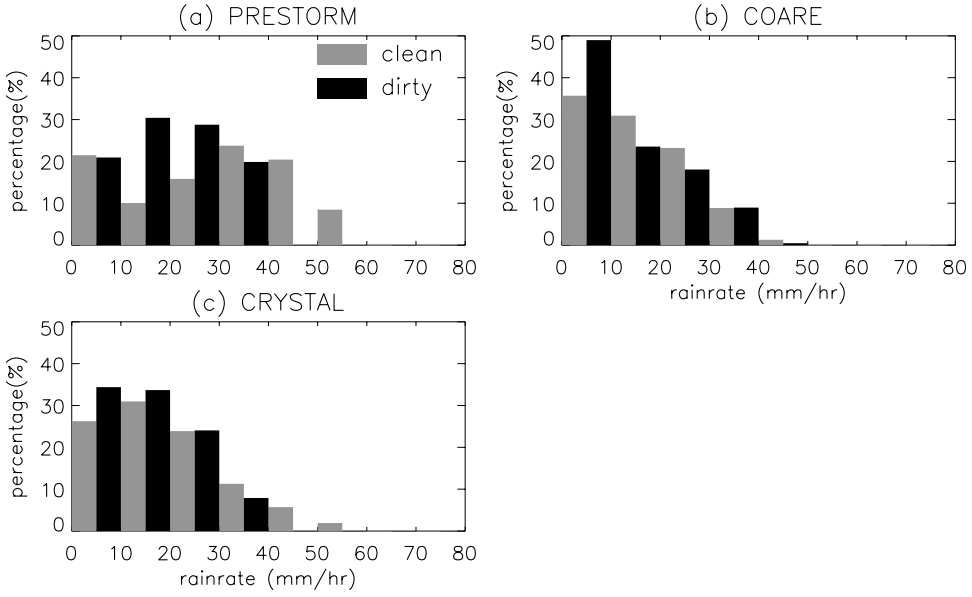

Figure 4. Probability distribution function of rainfall intensity for the (a) PRESTORM, (b) TOGA COARE, and (c) CRYSTAL cases. The gray and black bars represent clean and dirty conditions, respectively.

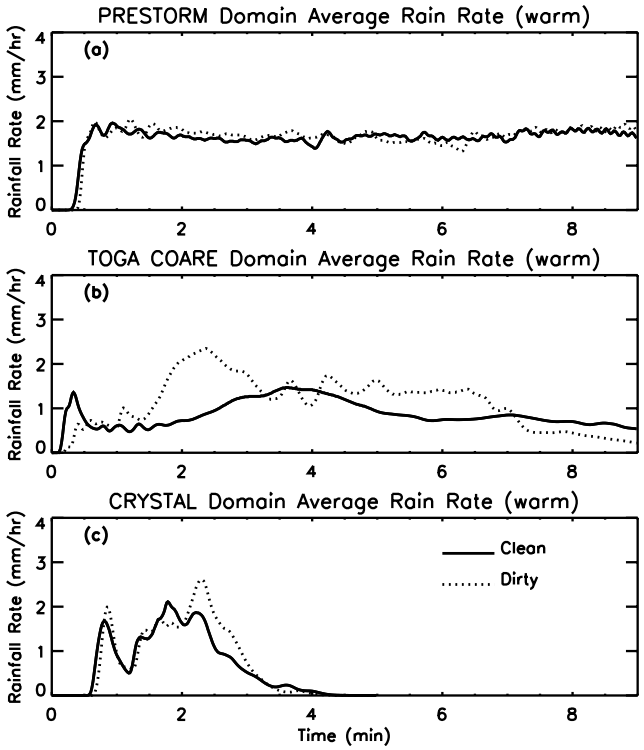

Figure 5. Same as Figure 2 except for sensitivity tests without ice processes (warm rain only): (a) PRESTORM, (b) TOGA COARE, and (c) CRYSTAL.

tests, the following microphysical processes are included: (1) condensation/evaporation of liquid drops, (2) drop/drop collision/coalescence, (3) turbulence effects on liquid drop collisions, (4) collisional breakup, and (5) sedimentation of liquid. These warm rain only sensitivity tests still allow condensation to occur above the freezing level, replacing the deposition. Therefore the differences between the pair of control runs (clean versus dirty) and the warm rain only runs can assess and examine the role of ice microphysics in producing the sensitivities between the clean and dirty environment.

[25] Figure 5 shows time sequences of GCE model-estimated domain mean surface rainfall rate without ice processes (warm rain only). For the PRESTORM case, the mean surface rainfall under both clean and dirty conditions is quite similar. The model-simulated maximum updraft velocity under clean and dirty conditions was also quite similar (Figure 6). The establishment of steady rain is also much faster compared with the full ice runs. This suggests that the ice processes are crucial in suppressing surface precipitation and increasing the portion of light rain in a dirty environment. For TOGA COARE, rain suppression due to high CCN is again only evident during the first hour of the simulations. For the entire period, increasing CCN still enhances rainfall; the same as with the full ice run. The maximum updraft velocity for the TOGA COARE case without ice processes (Figure 6) is also stronger in the dirty environment as with the ice case (Figure 3). These results suggest that ice processes do not have a major impact on the aerosol-precipitation interactions for the TOGA COARE case, because the majority of surface rainfall in this case comes from warm rain. Evaporative cooling and the strength of the cold pool, which affect cell regeneration in convective systems, are determined mainly by warm rain processes for the TOGA COARE case. (In spectral bin microphysics, water drops and their interactions with one another span the whole size spectrum. There is no clear distinction between cloud droplets and raindrops, and thus evaporative cooling comes from the entire size spectrum (i.e., from small cloud droplets to large precipitating rain drops).) Therefore the ice processes can only play a secondary role in terms of aerosol-precipitation interactions for the TOGA COARE case. For the CRYSTAL case, rainfall is enhanced with a high CCN. This enhancement is mainly associated with a relatively strong new cell generated at around t = 2.5 h. This may be caused by the enhanced evaporative cooling associated with the dirty case. These sensitivity tests also show the complexity of aerosol-precipitation interactions in mixed-phase, deep convection.

[26] Figure 7 shows the integrated total water and ice paths averaged every hour for clean and dirty conditions. The portions due to cloud water and pristine ice content are shown in hatched lines. For the PRESTORM case, the ice path is much larger than the liquid water path. More ice particles are produced by this convective system when a high CCN is assumed. The liquid water path is generally reduced with high CCN because smaller cloud particles have less chance of being collected compared to low-CCN conditions. Instead, more of them are transported above the freezing level and subsequently become ice particles in the dirty scenario. This is also why less rainfall reaches the ground for the high-CCN scenario in PRESTORM. For

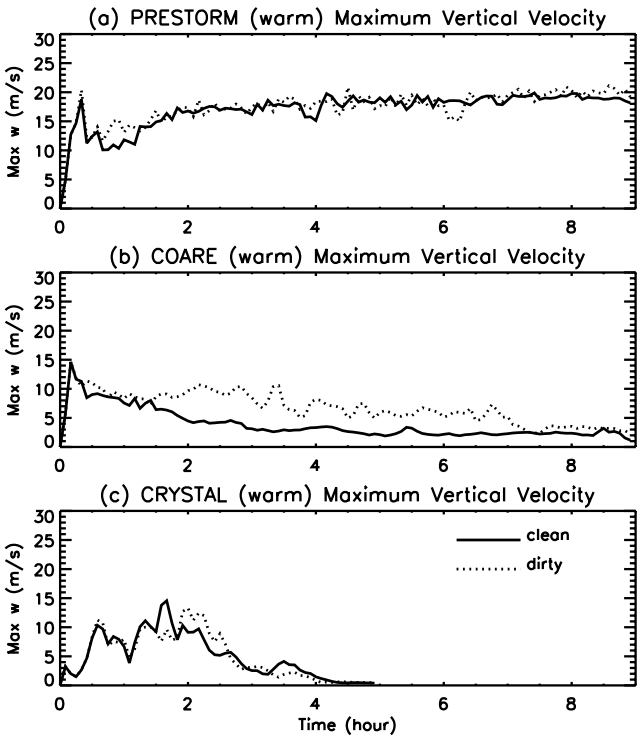

Figure 6. Same as Figure 3 except for sensitivity tests without ice processes (warm rain only): (a) PRESTORM, (b) TOGA COARE, and (c) CRYSTAL.

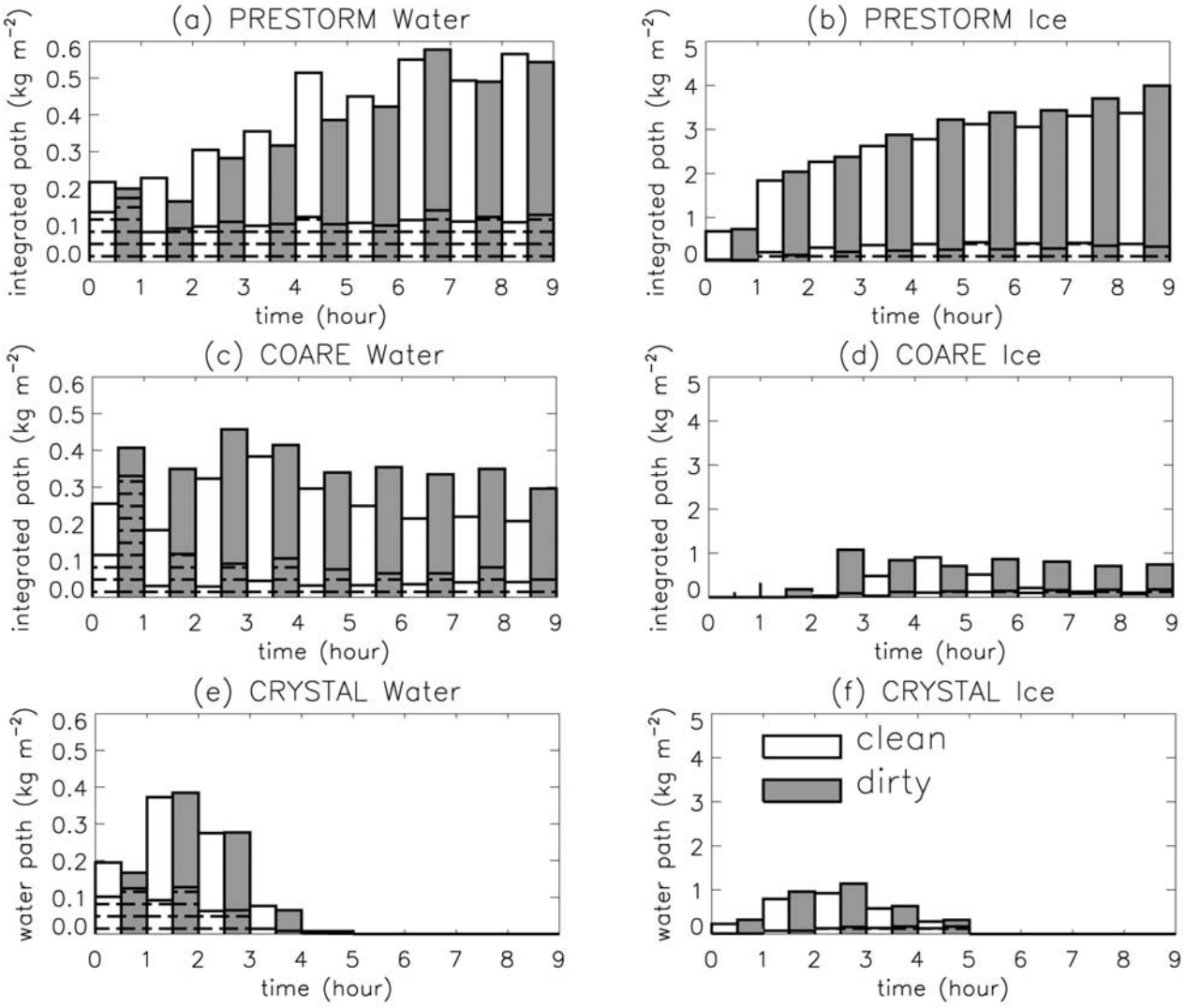

Figure 7. Integrated total water and ice path (kg m^{-2}) averaged every hour for clean (white) and dirty (gray) conditions: (a) PRESTORM water, (b) PRESTORM ice, (c) TOGA COARE water, (d) TOGA COARE ice, (e) CRYSTAL water, and (f) CRYSTAL ice. The hatched portion of each bar represents the cloud water and pristine ice content.

the TOGA COARE case, both liquid water path and ice water path increase when a high CCN is assumed. This is consistent with the more vigorous convection simulated in the dirty run. The ice path is still much smaller in this case than in the PRESTORM case. This is why the TOGA COARE case is less sensitive to ice processes compared with the PRESTORM case. More ice particles are also produced when a high CCN is assumed for the CRYSTAL-FACE case, but the differences are relatively small. As with the TOGA COARE case, the ice paths in CRYSTAL-FACE are much smaller than in the PRESTORM case. However, ice is produced at a very early stage in CRYSTAL-FACE as compared to TOGA COARE. This is why the CRYSTAL case is sensitive to ice processes.

[27] During the initial stages of cloud formation (the first and second hour), cloud water dominates the total liquid water path for the dirty runs, in contrast to the considerable amounts of rainwater in the clean runs. This again shows that rain formation is suppressed by increasing aerosols. However, this suppression becomes less obvious once the precipitation is well established, especially for the long-lived squall systems in PRESTORM and TOGA COARE.

[28] Figure 8 shows a schematic diagram of the physical processes that cause either enhancement (TOGA COARE) or suppression (PRESTORM) of precipitation in a dirty environment. In the early developing stages, small cloud droplets are produced in both the TOGA COARE and the PRESTORM cases with high CCN. Both cases also show narrower cloud drop size spectra for high CCN (not shown). This result is in good agreement with observations [i.e., *Twomey et al.*, 1984; *Albrecht*, 1989; *Rosenfeld*, 1999]. In this early stage, rain is suppressed for both cases with high CCN, which is also in good agreement with observations [e.g., *Rosenfeld*, 1999, 2000]. The suppression of precipitation in dirty conditions is mainly due to microphysical processes only. Smaller cloud droplets collide/coalesce less

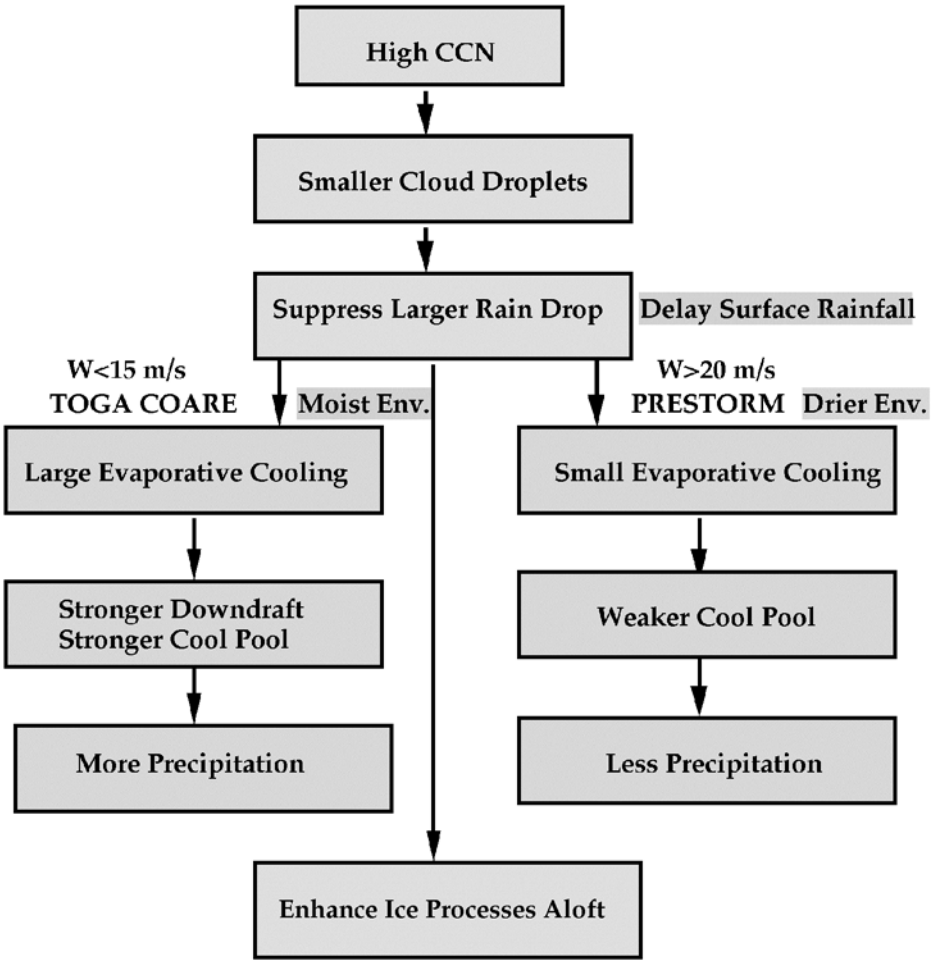

Figure 8. Schematic diagram showing the physical processes that lead to either enhancement (TOGA COARE case) or suppression (PRESTORM case) of precipitation in a dirty environment.

efficiently, delaying raindrop formation. These microphysical processes are very important especially in the early/developing stage of a cloud system.

[29] The model results also indicated that the low-level evaporative cooling is quite different between the clean and dirty case. Stronger evaporative cooling could enhance the near surface cold pool strength. When the cold pool interacts with the lower-level wind shear, the convergence could become stronger, producing stronger convection for the dirty cases. This can lead to more vigorous precipitation processes and therefore enhanced surface precipitation (positive feedback). Note that the enhanced precipitation can cause enhanced evaporation that in turn has a positive feedback on the rainfall amounts by triggering additional convection. These processes seem to be occurring in the TOGA COARE case, as shown in Figure 9a. In this case, evaporative cooling is more than twice as strong in the lower troposphere for the dirty scenario compared to the clean scenario. More rain reaches the surface after 30 min of model integration in the dirty case as compared to the clean case (Figure 2b). During this period, more evaporative cooling in the dirty case is already evident from the model results.

[30] On the other hand, evaporative cooling is stronger at lower levels in the clean scenario for the PRESTORM case (Figure 9b). This could be related to the early onset of rainfall in that run and because rain evaporation dominates the lower levels for this case. For the TOGA COARE case, the moist environment could inhibit evaporation of rain that forms early in the clean case. At higher levels in the PRESTORM case, cloud evaporation is still stronger for the dirty case as shown in Figure 9b. Note that the difference in the evaporative cooling between the dirty and clean runs in the PRESTORM case is smaller than that in the TOGA COARE case. The difference in the rainfall between the dirty and clean experiments in the PRESTORM case is also smaller than it is in the TOGA COARE case (Table 5).

[31] One main concern is the possibility of a cause-and-effect issue: namely, enhanced precipitation may enhance evaporation, which in turn can have a positive feedback on the rainfall amounts by triggering additional convection. Examination of the time series of evaporation rate in the TOGA COARE case shows that strong low-level evaporative cooling exists in the initial half hour for both the clean and dirty scenarios. The low-level evaporation is stronger in

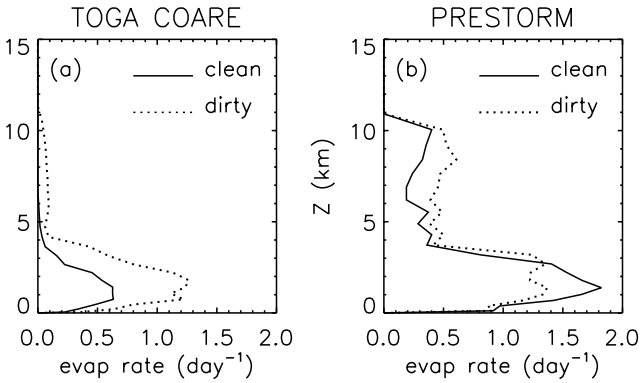

Figure 9. Domain average evaporation rate (d^{-1}) profiles during the first 2 h of model integration for the (a) TOGA COARE and (b) PRESTORM cases. The solid (dashed) line represents the dirty (clean) scenario.

the dirty case. The onset of surface rainfall comes after the initial half hour in the dirty case (see Figure 2) and clearly suggests that strong low-level evaporation precedes the onset of rainfall onset in the dirty case, which supports the schematic diagram (Figure 8).

[32] For all three cases, the dirty scenarios produce smaller cloud droplets with narrower spectrum, a delayed onset of rainfall, increased duration of diffusional droplet growth, increased latent heat release above the freezing level, and stronger vertical velocities at higher altitudes. The higher cloud tops, stronger updrafts, and deeper mixed-phase regions simulated in the dirty runs are in good agreement with observations (Table 1). The simulations all show that when the air is polluted, convection produces more ice particles, which is also in good agreement with observations. *van den Heever et al.* [2006] and *Carrio et al.* [2007] also found that smaller cloud droplets with a narrow spectrum delay the onset of rainfall, increase diffusional growth of droplets and enhance ice processes under dirty conditions (in agreement with the present study). This is potentially important for the formation and maintenance of high-altitude ice clouds in the anvil area, which in turn may play an important role in the Earth's radiation budget.

4. Comparison With Previous Modeling Studies

[33] Previous modeling studies have examined the role of aerosols on mixed-phase convective clouds for particular cases with different sets of model configurations and microphysics schemes (see Table 2). Although most of the model settings in those studies are not technically equivalent to this study, it is yet worthwhile to compare and review the different results. A simple metric, changes in time-integrated precipitation ($dP = 100 * (P_{dirty} - P_{clean})/P_{clean}$) as a result of increases in the number concentration of CCN ($dN_0 = N_{dirty} - N_{clean}$), is used to examine the different studies (Table 5).

[34] *Phillips et al.* [2002] is one of the earliest studies that applied an explicit microphysics module with a 2-D CRM to examine the influence of aerosol concentrations on a summertime cumulus cloud over New Mexico. The coupling is one way (i.e., the CRM provides dynamic input to the microphysics module). For a shallow cumulus (about 5 km cloud top), *Phillips et al.* [2002] found that with increased CCN, the precipitation rate, warm rain production, and secondary ice production are reduced. Although the sensitivity of ice microphysics to the aerosol number concentration appeared to be much less for the deep convective scenario than for the shallow convective cases, increasing the CCN from clean, unpolluted continental (N_0 = 800) to control (N_0 = 2750) and supercontinental

Table 5. Summary of Precipitation Sensitivity (dP) to Increases in the Number of CCN (dN_0) for Different Studies[a]

Reference	Case	$dN_0(N_{clean})$, cm^{-3}	dP, %
This study	TOGA COARE	2400 (100)	+58.
	PRESTORM	1900 (600)	−24.
	CRYSTAL	1900 (600)	−13.
Phillips et al. [2002]	New Mexico	1950 (800)	−14.
		4200 (800)	−30.
Khain et al. [2004]	GATE	1160 (100)	−3.
Khain and Pokrovsky [2004]	Texas	40 (10)	−16.
		90 (10)	−19.
		290 (10)	−53.
		1250 (10)	−88.
Khain et al. [2005]	PRESTORM	1160 (100)	+258.
Teller and Levin [2006]	Wintertime eastern Mediterranean	210 (100)	−27.
		510 (100)	−55.
		810 (100)	−73.
		1260 (100)	−93.
Wang [2005]	ITCZ	400(100)	+180.
		800 (100)	+340.
		1200(100)	+540.
		1500 (100)	+700.
Lynn et al. [2005a]	Florida	1250 (10)	−5.
van den Heever et al. [2006]	CRYSTAL	350 (300)	−22.

[a]Note that *van den Heever et al.* [2006] used a linear CCN concentration profile that ranged from 300 cm^{-3} at 4 km above ground level to 1000 cm^{-3} near the surface; GCCN and IN effects from *van den Heever et al.* [2006] and *Teller and Levin* [2006] are excluded from the table; only five of the total 30 cases from *Wang* [2005] are displayed in the table.

(N_0 = 5000) scenarios decreased the accumulated precipitation by 14% and 30%, respectively. In addition, the onset of precipitation is delayed by about 5 and 15 min, respectively, for the high-CCN scenarios in comparison with the low-CCN scenario.

[35] *Khain and Pokrovsky* [2004] and *Khain et al.* [2005] used a 2-D CRM with spectral microphysics (the same microphysics as used in this paper) to examine the aerosol impact on three deep convective clouds: an Atlantic squall line, an Oklahoma squall line (the same PRESTORM case in this paper), and a Texas convective cloud. Their results indicated that high CCN concentrations enhanced the precipitation processes for the Atlantic and Oklahoma squall line cases, but suppressed them for the Texas convective cloud. The results from *Khain and Pokrovsky* [2004] and *Khain et al.* [2005] also showed that high CCN could delay the warm rain process and enhance cold rain processes for all three cases. These features are also simulated in the present study. *Khain et al.* [2005] was the first modeling study to compute latent heat budget to examine the impact of aerosols on precipitation processes. For example, they found that for cases having suppressed precipitation with high CCN (the Texas convective cloud), a higher sublimation of ice and evaporation of drops (evaporative cooling) resulted in a higher loss of precipitation mass. The PRESTORM case simulated in this present paper also showed larger evaporative cooling aloft (5 km level or higher) with higher CCN. For cases having enhanced precipitation with high CCN (the Atlantic and Oklahoma squall lines), stronger updrafts/downdrafts and stronger convergence in the boundary layer may have enhanced the triggering of secondary clouds and produced a longer lifetime for the convective system. Stronger updrafts and downdrafts as well as more precipitation are also simulated in the current TOGA COARE case with high CCN. However, there is a significant difference between their study and this one for the PRESTORM case. With high CCN, *Khain et al.* [2005] were able to simulate a squall line for their PRESTORM case; with low CCN, they simulated a short-lived convective system rather than the observed squall line. The initial clouds (prior to the formation of secondary clouds or a squall line) produced more precipitation in the low-CCN case, in good agreement with the present study. The enhanced precipitation (dP = 258%) in the high-CCN case is due to the formation of the squall line during the 4 h of model integration time. The model dynamics (i.e., advection scheme and subgrid-scale turbulence) and setup (i.e., domain size, grid spacing, convective triggering) and lateral boundary condition used by *Khain et al.* [2005] and the present study are quite different. Some of these differences could explain the opposite impact of aerosol concentration on the PRESTORM squall line simulations. A pair of numerical experiments with higher horizontal spacing (500 m) for the PRESTORM case under clean and dirty conditions showed that increased aerosols suppressed precipitation [dP(%)] = −26% using 500 m resolution compared to −24% using 1000 m resolution.

[36] *Teller and Levin* [2006] used a 2-D CRM with spectral microphysics [*Reisin et al.*, 1998] to examine the aerosol impact on a winter convective cloud in the eastern Mediterranean region. Their results also showed that high CCN could delay rainfall and enhance cold rain processes. Their results also showed that larger number concentrations of CCN can decrease accumulated precipitation by 27% ∼ 93% over 80-min model integration. These features are also simulated in the present PRESTORM and CRYSTAL cases, though their simulation period is much shorter than this study. They also found that an increase in IN could reduce the total amount of precipitation but GCCN could enhance total precipitation in polluted clouds.

[37] *Wang* [2005] used a 3-D CRM with a two-moment bulk microphysical scheme to examine the aerosol impact on a convective system that developed in the ITCZ. His results showed that a high initial CCN concentration could produce stronger convection, more condensed cloud water mass, enhanced microphysical conversions, and more surface rainfall. *Wang* [2005] indicated that there are three processes by which precipitation is increased in tropical deep convection because of high CCN: (1) enhanced convective strength due to stronger and more latent heat release; (2) the dominant role of ice phase microphysics in rain production; and (3) greatly increased total water content in small liquid particles. The current tropical oceanic case (TOGA COARE) also produces stronger updrafts through more latent heat release aloft. However, ice processes are not the dominant rain-producing processes in this current tropical oceanic case (see the sensitivity test shown in Figure 5b). Differing dimensionalities, microphysical schemes, lateral boundary conditions (cyclic versus radiative open), and tropical cases (initial conditions) could explain the differences between the model results.

[38] *Lynn et al.* [2005a, 2005b] used spectral bin microphysics (a simplified version of Khain's scheme [*Khain et al.*, 2004]) and the fifth-generation Pennsylvania State University–National Center for Atmospheric Research (Penn State–NCAR) Mesoscale Model (MM5) to simulate a cloud that approached the west coast of Florida, prior to the sea breeze development on 27 July 1991. The use of a continental CCN concentration led to a delay in the growth of rainfall (in agreement with the present modeling study). The increase in CCN concentration led to convective invigoration and the formation of stronger secondary clouds [*Lynn et al.*, 2005b]. Simulations of rain events over the whole peninsula for this day showed significant invigoration of squall lines. There was an increase in precipitation rate and precipitation amount for a squall line that formed in the vicinity of the east coast of Florida. At the same time, continental CCN concentrations resulted in a 5% reduction in precipitation over the whole computational domain (containing a significant fraction of Florida) versus maritime values.

[39] *van den Heever et al.* [2006] used the Regional Atmospheric Modeling System (RAMS) and a two-moment bulk microphysical scheme [*Meyers et al.*, 1997; *Saleeby and Cotton*, 2004] to examine the aerosol effect on the formation of a thunderstorm over the peninsula of Florida (28 July 2002 during CRYSTAL-FACE). Note that the two-moment bulk scheme used by *van den Heever et al.* [2006] emulates a bin scheme by including explicit activation of aerosols [*Saleeby and Cotton*, 2004]. Sensitivity studies show that different combinations of CCN, GCCN, and IN result in different amounts and temporal patterns of cloud water/ice contents and rainfall. Their study showed that high

CCN reduce cumulative precipitation by 22% compared to low CCN. In addition, high GCCN and IN enhanced surface precipitation for the first 6 h of integration because of the initial broadening of the cloud droplet spectra. However, the total (12-h integration) accumulated precipitation was greatest for the clean (low CCN, GCCN, and IN) case. This could be explained by a rapid wet deposition of GCCN for the first 6 h of integration. All their experiments involving high CCN resulted in high cloud water content and weak surface precipitation. Using a similar modeling configuration, *van den Heever and Cotton* [2007] examine the sensitivity of urban-induced convective clouds over and downwind of St. Louis, MO. Their results indicate that downwind convergence (dynamic processes) induced by urban land cover appears to be the dominant factor in determining whether or not moist convection actually develops downwind of St, Louis. Once moist convection is initiated, urban-enhanced aerosols play a major role in determining the microphysical and dynamical characteristics of convective storms, particularly when background aerosol concentrations are low. Complicated relationships and feedbacks between microphysical and dynamical processes obscure generalized understandings (i.e., a linear relationship) of urban-enhanced aerosol effects on precipitation. Note that *van den Heever et al.* [2006] and *van den Heever and Cotton* [2007] explicitly represented mesoscale forcing (i.e., sea breeze convergence and urban heat island convergence). This is important because cold pools can interact with those circulations, introducing another level of dynamic complexity. For example, if the cold pools outrun those mesoscale convergence fields, precipitation is reduced whereas when they remain coupled precipitation is enhanced.

[40] Among these previous studies, the most striking difference is that cumulative precipitation can either increase or decrease in response to higher concentrations of CCN. *Khain and Pokrovsky* [2004] and *Teller and Levin* [2006] changed the number concentrations of CCN gradually and found robust decreases in cumulative precipitation for higher concentrations of CCN (Table 5). This is completely opposite from the result in *Wang* [2005]. Understanding these discrepancies is a necessary next step in resolving aerosol effects on cloud microphysics, dynamics and precipitation within climate systems.

5. Summary and Future Work

[41] A 2-D CRM with detailed spectral bin microphysics is used to examine the aerosol impact on deep convective clouds. Three cases are simulated using idealized initial aerosol concentrations: a case of sea breeze convection in Florida during CRYSTAL-FACE, a tropical mesosocale convective system during TOGA COARE, and a summertime midlatitude squall line during PRESTORM. Comparisons between the model simulations and in situ radar reflectivity observations show good agreements. A pair of model simulations, an experiment with low (clean) and an experiment with high CCN (dirty environment), is conducted for each case. The major highlights are as follows:

[42] 1. For all three cases, higher CCN produces smaller cloud droplets and a narrower spectrum. Dirty conditions delay rain formation, increase latent heat release above the freezing level, and enhance vertical velocities at higher altitude for all cases. Stronger updrafts, deeper mixed-phase regions, and more ice particles are simulated with higher CCN in good agreement with observations.

[43] 2. In all cases, rain reaches the ground early with lower CCN. Rain suppression is also evident in all three cases with high CCN in good agreement with observations (*Rosenfeld*, 1999, 2000 and others). Rain suppression, however, only occurs during the first hour of simulation. This result suggests that microphysical processes dominate the impact of aerosols on precipitation in the early stage of precipitation development.

[44] 3. During the mature stage of the simulations, the effect of increasing aerosol concentration ranges from rain suppression in the PRESTORM case to little effect on surface rainfall in the CRYSTAL-FACE case to rain enhancement in the TOGA COARE case.

[45] 4. The model results suggest that evaporative cooling is a key process in determining whether higher CCN reduces or enhances precipitation. Cold pool strength can be enhanced by stronger evaporation. When cold pool interacts with the near surface wind shear, the low-level convergence can be stronger, facilitating secondary cloud formation and more vigorous precipitation processes. Evaporative cooling is more than two times stronger at low levels with higher CCN for the TOGA COARE case during the early stages of precipitation development. However, evaporative cooling is slightly stronger at lower levels with lower CCN for the PRESTORM case. The early formation of rain in the clean environment could allow for the formation of an earlier and stronger cold pool compared to a dirty environment. PRESTORM has a very dry environment and both large and small raindroplets can evaporate. Consequently, the cold pool is relatively weaker, and the system is relatively less intense with higher CCN.

[46] 5. Sensitivity tests are conducted to determine the impact of ice processes on aerosol-precipitation interaction. The results suggested that ice processes are crucial for suppressing precipitation because of high CCN for the PRESTORM case. More and smaller ice particles are generated in the dirty case and transported to the trailing stratiform region. This reduces the heavy convective rain and contributes to the weakening of the cold pool. Warm rain processes dominate the TOGA COARE case. Therefore ice processes only play a secondary role in terms of aerosol-precipitation interaction.

[47] 6. Two of the three cloud systems presented in this paper formed a line structure (squall system). A 2-D simulation therefore gives a good approximation to such a line of convective clouds. Since the real atmosphere is 3-D, further 3-D cloud-resolving simulations are needed to address aerosol-precipitation interactions.

[48] Most previous modeling results found that high CCN concentrations could suppress precipitation processes [i.e., *Khain et al.*, 2004, 2005; *Cheng et al.*, 2007, *Lynn et al.*, 2005b; *van den Heever et al.*, 2006; *Teller and Levin*, 2006; *van den Heever and Cotton*, 2007]. However, high CCN concentrations could also enhance precipitation processes [*Wang*, 2005; *Khain et al.*, 2005]. These results show the complexity of aerosol interactions with convection. More case studies are required to further investigate the aerosol impact on rain events. In almost all previous cloud-resolving modeling studies (including the present study),

idealized or composite [i.e., *van den Heever et al.*, 2006] CCN concentrations were used in the model simulations. A horizontally uniform distribution of CCN was also used in the mesoscale modeling studies. A nonhomogeneous CCN distribution, consistent with the nonhomogeneous initial meteorological conditions, will be required to assess aerosol-precipitation interactions using regional-scale models in the future. In addition to IN and GCCN, the chemistry of CCN needs to be considered in future modeling of aerosol-precipitation interactions. For example, *Fan et al.* [2007] and *Ekman et al.* [2004, 2006] found that aerosol chemical composition and aerosol physics could affect precipitation processes.

[49] Many previous CRM studies did not compare model results with observed cloud structures, organization, radar reflectivity and rainfall. Some of the CRM domains were too small to resolve the observed clouds or precipitation systems (the domain size has to be at least twice as large as the simulated features). It may require major field campaigns to gather the data necessary to both initialize (with meteorological and aerosol) and validate (i.e., in situ cloud property observations, radar, lidar, and microwave remote sensing) the models. Although CRM-simulated results can provide valuable quantitative estimates of the indirect effects of aerosols, CRMs are neither regional nor global models and can only simulate clouds and cloud systems over a relatively small domain. Close collaboration between the global and CRM communities is needed in order to expand the CRM results to a regional and global perspective [*Tao et al.*, 2003b].

[50] **Acknowledgments.** The GCE model is mainly supported by the NASA Headquarters Atmospheric Dynamics and Thermodynamics Program and the NASA Tropical Rainfall Measuring Mission (TRMM). The authors are grateful to R. Kakar at NASA headquarters for his support of this research. A. Khain was supported by the European "ANTISTORM" project. We also thank W. Cotton, C. Wang, and D. Rosenfeld for their constructive comments that improved this paper significantly. The research was also supported by the Office of Science (BER), U.S. Department of Energy/Atmospheric Radiation Measurement (DOE/ARM) Interagency Agreement DE-AI02-04ER63755. The authors are grateful to Kiran Alapaty at DOE/ARM for his support of this research. The authors acknowledge NASA Goddard Space Flight Center for computer time used in this research.

References

Ackerman, A. S., O. B. Toon, D. E. Stevens, A. J. Heymsfield, V. Ramanathan, and E. J. Welton (2000), Reduction of tropical cloudiness by soot, *Science*, *288*, 1042–1047.

Albrecht, B. A. (1989), Aerosols, cloud microphysics and fractional cloudiness, *Science*, *245*, 1227–1230.

Andreae, M. O., D. Rosenfeld, P. Artaxo, A. A. Costa, G. P. Frank, K. M. Longo, and M. A. F. Silva-Dias (2004), Smoking rain clouds over the Amazon, *Science*, *303*, 1337–1342.

Bell, T. L., D. Rosenfeld, K.-M. Kim, J.-M. Yoo, M.-I. Lee, and M. Hahnenberger (2007), Midweek increase in U.S. summer rain and storm heights suggests air pollution invigorates rainstorms, *J. Geophys. Res.*, doi:10.1029/2007JD008623, in press.

Carrio, G. G., S. C. van den Heever, and W. R. Cotton (2007), Impact of nucleating aerosol on anvil-cirrus clouds: A modeling study, *Atmos. Res.*, *84*, 111–131.

Cheng, C.-T., W.-C. Wang, and J.-P. Chen (2007), A modeling study of aerosol impacts on cloud microphysics and radiative properties, *Q. J. R. Meteorol. Soc.*, *133*, 283–297.

Chou, M.-D. and M. J. Suarez (1994), An efficient thermal infrared radiation parameterization for use in general circulation models, *NASA Tech. Memo.*, *104606*, 85 pp.

Chou, M.-D., M. J. Suarez, C.-H. Ho, M.-H. Yan, and K.-T. Lee (1998), Parameterizations for cloud overlapping and shortwave single-scattering properties for use in general circulation and cloud ensemble models, *J. Clim.*, *11*, 202–214.

Cooper, W. A., R. Bruintjes, and G. Mather (1997), Calculations pertaining to hygroscopic seeding with flares, *J. Appl. Meteorol.*, *36*, 1449–1469.

Ekman, A., C. Wang, J. Wilson, and J. Strom (2004), Explicit simulation of aerosol physics in a cloud-resolving model: A sensitivity study based on an observed convective cloud, *Atmos. Chem. Phys.*, *4*, 773–791.

Ekman, A., C. Wang, J. Storm, and R. Kreici (2006), Explicit simulation of aerosol physics in a cloud-resolving model: Aerosol transport and processing in the free troposphere, *J. Atmos. Sci.*, *63*, 682–696.

Fairall, C. W., E. F. Bradley, D. P. Rogers, J. B. Edson, and G. S. Young (1996), Bulk parameterization of air-sea fluxes for Tropical Ocean-Global Atmosphere Coupled Ocean-Atmosphere Response Experiment, *J. Geophys. Res.*, *101*, 915–929.

Fan, J., R. Zhang, G. Li, W.-K. Tao, and X. Li (2007), Simulations of cumulus clouds using a spectral microphysics cloud-resolving model, *J. Geophys. Res.*, *112*, D04201, doi:10.1029/2006JD007688.

Ferrier, B. S., J. Simpson, and W.-K. Tao (1996), Factors responsible for precipitation efficiencies in midlatitude and tropical squall simulations, *Mon. Weather Rev.*, *124*, 2100–2125.

Fovell, R. G., and Y. Ogura (1988), Numerical simulation of a midlatitude squall line in two dimensions, *J. Atmos. Sci.*, *45*, 3846–3879.

Fridlind, A. M., et al. (2004), Evidence for the predominance of mid-tropospheric aerosols as subtropical anvil cloud nuclei, *Science*, *304*, 718–722.

Hallett, J., and S. C. Mossop (1974), Production of secondary ice crystals during the riming process, *Nature*, *249*, 26–28.

Heymsfield, G. M., A. J. Heymsfield, and L. Belcher (2004), Observations of Florida convective storms using dual wavelength airborne radar, paper presented at International Conference on Clouds and Precipitations, Inst. of Atmos. Sci. and Clim., Bologna, Italy, 18–23 July.

Hudson, J. G. (1984), Cloud condensation nuclei measurements within clouds, *J. Clim. Appl. Meteorol.*, *23*, 42–51.

Hudson, J. G. (1993), Cloud condensation nuclei near marine cumulus, *J. Geophys. Res.*, *98*, 2693–2701.

Johnson, R. H., and P. J. Hamilton (1988), The relationship of surface pressure features to the precipitation and airflow structure of an intense midlatitude squall line, *Mon. Weather Rev.*, *116*, 1444–1472.

Jorgensen, D. P., M. A. LeMone, and S. B. Trier (1997), Structure and evolution of the 22 February 1993 TOGA COARE squall line: Aircraft observations of precipitation, circulation, and surface fluxes, *J. Atmos. Sci.*, *54*, 1961–1985.

Khain, A., and A. Pokrovsky (2004), Simulation of effects of atmospheric aerosols on deep turbulent convective clouds using a spectral microphysics mixed-phase cumulus cloud model. part II: Sensitivity study, *J. Atmos. Sci.*, *61*, 2963–2982.

Khain, A., M. Ovtchinnikov, M. Pinsky, A. Podrovsky, and H. Krugliak (2000), Notes on the state-of-art numerical modeling of cloud microphysics, *Atmos. Res.*, *55*, 159–224.

Khain, A., A. Pokrovsky, M. Pinsky, A. Seigert, and V. Phillips (2004), Simulation of effects of atmospheric aerosols on deep turbulent convective clouds using a spectral microphysics mixed-phase cumulus cloud model. part I: Model description and possible applications, *J. Atmos. Sci.*, *61*, 2983–3001.

Khain, A., D. Rosenfeld, and A. Pokrovsky (2005), Aerosol impact on the dynamics and microphysics of deep convective clouds, *Q. J. R. Meteorol. Soc.*, *131*, 1–25.

Klemp, J. B., and R. B. Wilhelmson (1978), The simulation of three-dimensional convective storm dynamics, *J. Atmos. Sci.*, *35*, 1070–1096.

Koren, I., Y. J. Kaufman, D. Rosenfeld, L. A. Remer, and Y. Rudich (2005), Aerosol invigoration and restructuring of Atlantic convective clouds, *Geophys. Res. Lett.*, *32*, L14828, doi:10.1029/2005GL023187.

Lang, S., W.-K. Tao, J. Simpson, and B. Ferrier (2003), Modeling of convective-stratiform precipitation processes: Sensitivity to partitioning methods, *J. Appl. Meteorol.*, *42*, 505–527.

LeMone, M. A., D. P. Jorgensen, and B. F. Smull (1994), The impact of two convective systems of sea surface stresses in COARE, paper presented at Sixth Conference on Mesoscale Processes, Am. Meteorol. Soc., Portland, Oreg.

Lin, J. C., T. Matsui, R. A. Pielke Sr., and C. Kummerow (2006), Effects of biomass-burning-derived aerosols on precipitation and clouds in the Amazon Basin: a satellite-based empirical study, *J. Geophys. Res.*, *111*, D19204, doi:10.1029/2005JD006884.

Lynn, B. H., A. Khain, J. Dudhia, D. Rosenfeld, A. Pokrovsky, and A. Seifert (2005a), Spectral (bin) microphysics coupled with a mesoscale model (MM5) part I: Model description and first results, *Mon. Weather Rev.*, *133*, 44–58.

Lynn, B. H., A. Khain, J. Dudhia, D. Rosenfeld, A. Pokrovsky, and A. Seifert (2005b), Spectral (bin) microphysics coupled with a mesoscale

model (MM5) part II: Simulation of a CaPE rain event with a squall line, *Mon. Weather Rev.*, *133*, 59–71.
Meyers, M. P., P. J. DeMott, and W. R. Cotton (1992), New primary ice-nucleation parameterization in an explicit cloud model, *J. Appl. Meteorol.*, *31*, 708–721.
Meyers, M. P., R. L. Walko, J. Y. Harrington, and W. R. Cotton (1997), New RAMS cloud microphysics parameterization. part II: The two-moment scheme, *Atmos. Res.*, *45*, 3–39.
Mossop, S. C., and J. Hallett (1974), Ice crystal concentration in cumulus clouds: Influence of the drop spectrum, *Science*, *186*, 632–634.
National Research Council (2005), *Radiative Forcing of Climate Change: Expanding the Concept and Addressing Uncertainties*, Natl. Acad., Washington, D. C.
Orville, R. E., R. Zhang, J. N. Gammon, D. Collins, B. Ely, and S. Steiger (2001), Enhancement of cloud-to-ground lightening over Houston, Texas, *Geophys. Res. Lett.*, *28*, 2597–2600.
Phillips, V. T. J., T. W. Choularton, A. M. Blyth, and J. Latham (2002), The influence of aerosol concentrations on the glaciation and precipitation of a cumulus cloud, *Q. J. R. Meteorol. Soc.*, *128*, 951–971.
Pinsky, M., A. P. Khain, and M. Shapiro (2000), Stochastic effect on cloud droplet hydrodynamic interaction in a turbulent flow, *Atmos. Res.*, *53*, 131–169.
Pinsky, M., A. P. Khain, and M. Shapiro (2001), Collision efficiency of drops in a wide range of Reynolds numbers: Effects of pressure on spectrum evolution, *J. Atmos. Sci.*, *58*, 742–764.
Pruppacher, H. R. and J. D. Klett (1997), *Microphysics of Clouds and Precipitation*, 2nd ed., 914 pp., Oxford Univ. Press, New York.
Ramanathan, V., P. J. Crutzen, J. T. Kiehl, and D. Rosenfeld (2001), Aerosols, climate, and the hydrological cycle, *Science*, *294*, 2119–2124.
Redelsperger, J.-L., et al. (2000), A GCSS model intercomparison for a tropical squall line observed during TOGA-COARE. part I: Cloud-resolving models, *Q. J. R. Meteorol. Soc.*, *126*, 823–863.
Reisin, T. G., Y. Yin, Z. Levin, and S. Tzivion (1998), Development of giant drops and high reflectivity cores in Hawaiian clouds: Numerical simulation using a kinematic model with detailed microphysics, *Atmos. Res.*, *45*, 275–297.
Ridley, B., et al. (2004), Florida thunderstorms: A faucet of reactive nitrogen to the upper troposphere, *J. Geophys. Res.*, *109*, D17305, doi:10.1029/2004JD004769.
Rosenfeld, D. (1999), TRMM observed first direct evidence of smoke from forest fires inhibiting rainfall, *Geophys. Res. Lett.*, *26*, 3105–3108.
Rosenfeld, D. (2000), Suppression of rain and snow by urban and industrial air pollution, *Science*, *287*, 1793–1796.
Rosenfeld, D., and I. Lensky (1998), Satellite-based insights into precipitation formation processes in continental and maritime convective clouds, *Bull. Am. Meteorol. Soc.*, *79*, 2457–2476.
Rosenfeld, D. and C. W. Ulbrich (2003), Cloud microphysical properties, processes, and rainfall estimation opportunities, in *Radar and Atmospheric Science: A Collection of Essays in Honor of David Atlas*, edited by Roger M. Wakimoto and Ramesh Srivastava, *Meteorol. Monogr.*, *52*, 237–258.
Rosenfeld, D., and W. L. Woodley (2000), Convective clouds with sustained highly supercooled liquid water down to −37°C, *Nature*, *405*, 440–442.
Rosenfeld, D., Y. Rudich, and R. Lahav (2001), Desert dust suppressing: A possible desertification feedback loop, *Proc. Natl. Acad. Sci. U.S.A.*, *98*, 5975–5980.
Rutledge, S. A., R. A. Houze Jr., and M. I. Biggerstaff (1988), The Oklahoma-Kansas mesoscale convective system of 10–11 June 1985: Precipitation structure and single-Doppler radar analysis, *Mon. Weather Rev.*, *116*, 1409–1430.
Saleeby, S. M., and W. R. Cotton (2004), A large-droplet mode and prognostic number concentration of cloud droplets in the Colorado State Univ. Regional Atmospheric Modeling System (RAMS). part I: Module descriptions and supercell test simulations, *J. Appl. Meteorol.*, *43*, 182–195.
Seifert, A., A. Khain, U. Blahak, and K. D. Beheng (2005), Possible effects of collisional breakup on mixed-phase deep convection simulated by a spectral (bin) cloud model, *J. Atmos. Sci.*, *62*, 1917–1931.
Shepherd, J. M. (2005), A review of current investigations of urban-induced rainfall and recommendations for the future, *Earth Interactions*, *9*, 1–27.
Smolarkiewicz, P. K., and W. W. Grabowski (1990), The multidimensional positive advection transport algorithm: Nonoscillatory option, *J. Comput. Phys.*, *86*, 355–375.
Soong, S.-T., and Y. Ogura (1980), Response of trade wind cumuli to large-scale processes, *J. Atmos. Sci.*, *37*, 2035–2050.
Soong, S.-T., and W.-K. Tao (1980), Response of deep tropical clouds to mesoscale processes, *J. Atmos. Sci.*, *37*, 2016–2034.
Squires, P. and T. Twomey (1960), The relation between cloud drop numbers and the spectrum of cloud nuclei, in *Physics of Precipitation*, *Geophys. Monogr. Ser.*, vol. 5, edited by H. Weickmann, pp. 211–219, AGU, Washington, D. C.
Sui, C.-S., X. Li, and M.-J. Yang (2007), On the definition of precipitation efficiency, *J. Atmos. Sci.*, in press.
Tao, W.-K., and J. Simpson (1993), Goddard cumulus ensemble model. part I: Model description, *Terr. Atmos. Oceanic Sci.*, *4*, 35–72.
Tao, W.-K., J. Simpson, C.-H. Sui, B. Ferrier, S. Lang, J. Scala, M.-D. Chou, and K. Pickering (1993), Heating, moisture and water budgets of tropical and midlatitude squall lines: Comparisons and sensitivity to longwave radiation, *J. Atmos. Sci.*, *50*, 673–690.
Tao, W.-K., J. Scala, and J. Simpson (1995), The effects of melting processes on the development of a tropical and a midlatitude squall line, *J. Atmos. Sci.*, *52*, 1934–1948.
Tao, W.-K., S. Lang, J. Simpson, C.-H. Sui, B. Ferrier, and M.-D. Chou (1996), Mechanisms of cloud-radiation interaction in the tropics and midlatitudes, *J. Atmos. Sci.*, *53*, 2624–2651.
Tao, W.-K., et al. (2003a), Microphysics, radiation and surface processes in the Goddard cumulus ensemble (GCE) model, *Meteorol. Atmos. Phys.*, *82*, 97–137.
Tao, W.-K., D. Starr, A. Hou, P. Newman, and Y. Sud (2003b), A cumulus parameterization workshop, *Bull. Am. Meteorol. Soc*, *84*, 1055–1062.
Teller, A., and Z. Levin (2006), The effects of aerosols on precipitation and dimensions of subtropical clouds: A sensitivity study using a numerical cloud model, *Atmos. Chem. Phys.*, *6*, 67–80.
Trier, S. B., W. C. Skamarock, M. A. LeMone, D. B. Parsons, and D. P. Jorgensen (1996), Structure and evolution of the 22 February 1993 TOGA COARE squall line: Numerical simulations, *J. Atmos. Sci.*, *53*, 2861–2886.
Trier, S. B., W. C. Skamarock, and M. A. LeMone (1997), Structure and evolution of the 22 February 1993 TOGA COARE squall line: Organization mechanisms inferred from numerical simulation, *J. Atmos. Sci.*, *54*, 386–407.
Twomey, S. A. (1977), The influence of pollution on the shortwave albedo of clouds, *J. Atmos. Sci.*, *34*, 1149–1152.
Twomey, S., and T. A. Wojciechowski (1969), Observations of the geographical variation of cloud nuclei, *J. Atmos. Sci.*, *26*, 684–688.
Twomey, S. A., M. Piepgrass, and T. L. Wolfe (1984), An assessment of the impact of pollution on global cloud albedo, *Tellus, Ser. B*, *36*, 356–366.
Vali, G. (1994), Freezing rate due to heterogeneous nucleation, *J. Atmos. Sci.*, *51*, 1843–1856.
van den Heever, S. C., and W. R. Cotton (2007), Urban aerosol impacts on downwind convective storms, *J. Appl. Meteorol. Clim.*, *46*, 828–850.
van den Heever, S. C., G. G. Carrió, W. R. Cotton, P. J. DeMott, and A. J. Prenni (2006), Impact of nucleating aerosol on Florida storms. part 1: Mesoscale simulations, *J. Atmos. Sci.*, *63*, 1752–1775.
Wang, C. (2005), A modeling study of the response of tropical deep convection to the increase of cloud condensation nuclei concentration: 1. Dynamics and microphysics, *J. Geophys. Res.*, *110*, D21211, doi:10.1029/2004JD005720.
Wang, Y., W.-K. Tao, and J. Simpson (1996), The impact of a surface layer on a TOGA COARE cloud system development, *Mon. Weather Rev.*, *124*, 2753–2763.
Wang, Y., W.-K. Tao, J. Simpson, and S. Lang (2003), The sensitivity of tropical squall lines to surface fluxes: Three-dimensional cloud resolving model simulations, *Q. J. R. Meteorol. Soc.*, *129*, 987–1006.
Warner, J. (1968), A reduction in rainfall associated with smoke from sugarcane fires: An inadvertent weather modification?, *J. Appl. Meteorol.*, *7*, 247–251.
Warner, J., and S. Twomey (1967), The production of cloud nuclei by cane fires and the effects on cloud droplet concentration, *J. Atmos. Sci.*, *24*, 704–706.
Williams, E., et al. (2002), Contrasting convective regimes over the Amazon: Implications for cloud electrification, *J. Geophys. Res.*, *107*(D20), 8082, doi:10.1029/2001JD000380.
Yang, M.-J., and R. A. Houze Jr. (1995), Multicell squall-line structure as a manifestation of vertically trapped gravity waves, *Mon. Weather Rev.*, *123*, 641–661.

A. Khain, Department of Atmospheric Science, Hebrew University of Jerusalem, Jerusalem 91904, Israel.
S. Lang, Science Systems and Applications, Inc., Lanham, MD 20706, USA.
X. Li, T. Matsui, J. Simpson, and W.-K. Tao, Laboratory for Atmospheres, NASA Goddard Space Flight Center, Greenbelt, MD 20771, USA. (tao@agnes.gsfc.nasa.gov)